Technetium-99m-HMPAO SPECT in Sturge-Weber Syndrome

Zvi Bar-Sever, Leonard P. Connolly, Patrick D. Barnes and S. Ted Treves
Divisions of Nuclear Medicine and Neuroradiology, Department of Radiology, Children's Hospital, Harvard Medical School, Boston, Massachusetts

Technetium-99m-HMPAO interictal SPECT was performed on three pediatric patients with Sturge-Weber syndrome (SWS). **Results:** Brain SPECT of all three patients demonstrated markedly diminished tracer localization in the affected hemisphere. In one patient, the SPECT abnormality was more extensive than the associated abnormalities on CT and MRI. **Conclusion:** Technetium-99m-HMPAO brain SPECT can detect cerebral perfusion abnormalities associated with SWS and deserves consideration in the imaging evaluation of SWS patients.

Key Words: technetium-99m-HMPAO; SPECT; Sturge-Weber syndrome; brain

J Nucl Med 1996; 37:81–83

Sturge-Weber syndrome (SWS) is a rare nonhereditary neurocutaneous disorder. The characteristic anatomic abnormalities are facial angioma, known as port wine stain, and an ipsilateral cerebral leptomeningeal venous angioma. Patients are usually asymptomatic during the first months of life but typically develop seizures during the following 3 yr. These seizures are often refractory to medical therapy, in which case hemispherectomy or a more limited surgical resection may be indicated (*1*). Additional clinical manifestations include hemiparesis contralateral to the pial angioma, intellectual impairment, homonymous hemianopsia, glaucoma and transient ischemic episodes (*2–5*).

The diagnosis of SWS is based on clinical and radiological findings. CT and MRI are the imaging modalities most frequently used in the diagnosis and follow-up of SWS. We report the ^{99m}Tc-hexamethylpropylene amine oxime (HMPAO) SPECT findings of three patients with SWS.

CASE REPORTS

Patient 1

A prominent port wine nevus was noted on the left forehead of a male infant delivered at the completion of an uncomplicated full-term pregnancy. He was asymptomatic until 5 mo of age when he developed right-sided tonic clonic seizures. CT scans (Fig. 1A) revealed minimal prominence of the left frontal sulci and subtle high density of the left parietal gyri. The seizures gradually became refractory to medical treatment. Over the next 2 yr of life, he experienced progressive neurological deterioration that included right-sided hemiparesis, homonymous hemianopsia and developmental delay. CT (Fig. 1B) performed at 22 mo demonstrated widespread calcifications in the left cerebral hemisphere as well as diffuse cortical atrophy on the left. Gadolinium-enhanced MRI (Fig. 1C, D) demonstrated marked left cortical atrophy and enhancement. An electroencephalogram (EEG) showed epileptic activity originating from the left cerebral cortex. The clinical and radiological findings led to a diagnosis of SWS. Interictal ^{99m}Tc HMPAO SPECT (Fig. 1E, F) demonstrated marked cortical hypoperfusion involving the entire left hemisphere. The patient underwent left hemispherectomy at 25 mo of age and has had a favorable postoperative course without further seizures.

Received Apr. 19, 1995; revision accepted May 15, 1995.
For correspondence or reprints contact: S. Ted Treves, MD, Division of Nuclear Medicine, Department of Radiology, Children's Hospital, 300 Longwood Ave., Boston, MA 02115.

Patient 2

At birth, a male infant was observed as having a prominent port wine nevus of the right face, which extended into the neck, shoulder, trunk, right upper extremity and the left portion of his face. At 6 mo of age, the infant developed left-sided motor seizures. CT revealed a subtle degree of left cerebral atrophy. Based on the clinical and radiological findings, a diagnosis of SWS was made. The seizures became refractory to anticonvulsant therapy. The child developed left hemiparesis and was developmentally delayed. Gadolinium-enhanced MRI at 16 mo (Fig. 2A) revealed right hemispheric atrophy and cortical enhancement. Interictal ^{99m}Tc-HMPAO SPECT (Fig. 2B, C) demonstrated marked hypoperfusion of the entire right cerebral cortex. He underwent right hemispherectomy and has experienced complete cessation of seizures during the postoperative period.

Patient 3

A male infant, born following a normal pregnancy and delivery, was observed to have a right facial port wine stain and right-sided buphthalmos. At 1 yr, he developed a seizure disorder. Several seizure types, mostly partial complex, were observed. An EEG showed baseline depressed activity on the right with occasional spikes over the central and temporal areas. CT revealed right cerebral atrophy and extensive right hemispheric calcifications, predominantly located in the frontal and occipital lobes. A diagnosis of SWS was made. His seizures were controlled with anticonvulsives during childhood and he experienced no significant neurological deficits. He subsequently developed a learning disability and his seizures worsened during early adolescence. At age 11, CT (Fig. 3A) showed no change in the cerebral calcifications or atrophy. MRI at age 14 (Fig. 3B) revealed progression of the hemiatrophy. Interictal ^{99m}Tc-HMPAO SPECT (Fig. 3C, D) demonstrated marked hypoperfusion of the right occipital, parietal and posterior frontal cortex. These findings were more extensive than the abnormalities observed on MRI. He continues to receive medical treatment.

Imaging Technique

Each patient was injected interictally with ^{99m}Tc-HMPAO (11 MBq/kg). Images were acquired 30 min later with each patient sedated and under constant monitoring of vital signs. Brain SPECT was performed with a triple-head camera equipped with a high-resolution collimator. Each patient was positioned supine with the head positioned and secured between the collimators with the aid of laser guides and headholders. A total of 120 views were acquired (40 stops) and recorded on a 128 × 128 matrix. The images were reconstructed, corrected for attenuation and realigned.

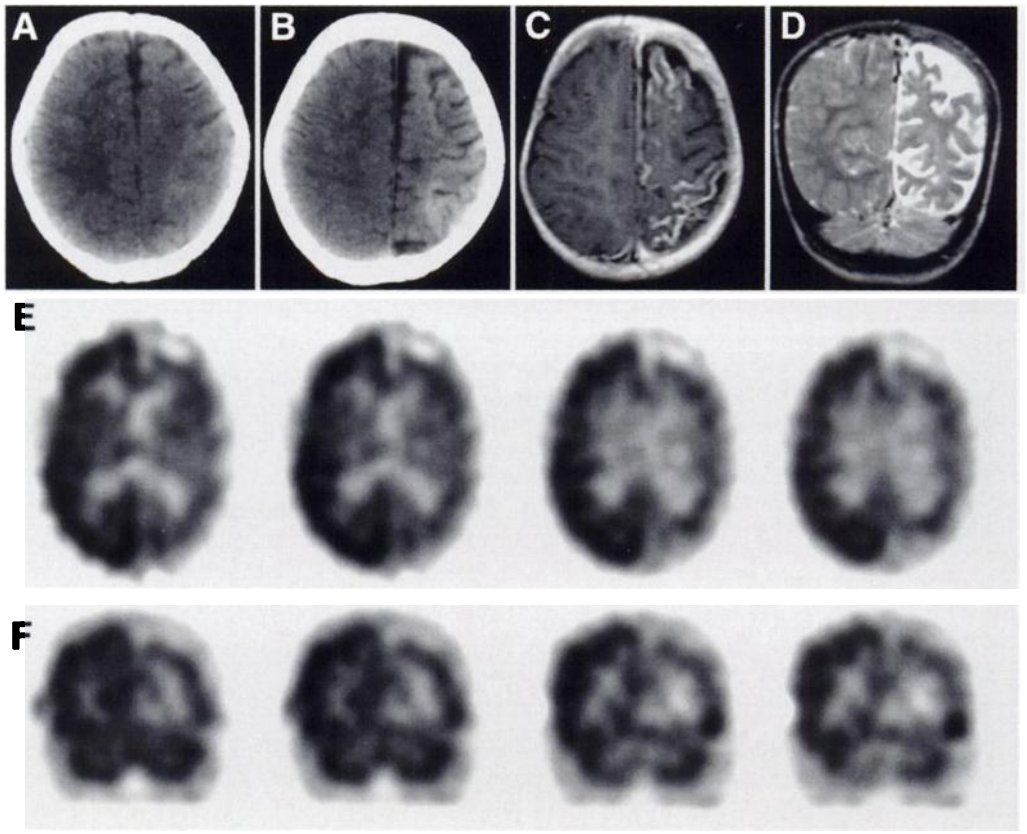

FIGURE 1. Nonenhanced CT (A) performed at age 5 mo reveals minimal prominence of the left frontal sulci and subtle high density of the parietal gyri. Nonenhanced CT (B) at age 22 mo demonstrates progressive sulcal widening and high-density calcifications. Gadolinium-enhanced, T1-weighted axial (C) and T2-weighted coronal MRI (D) show left frontal and parietal cortical enhancement and cortical atrophy. Transverse (E) and coronal (F) ^{99m}Tc-HMPAO SPECT reveal markedly diminished tracer localization in the left cerebral hemisphere.

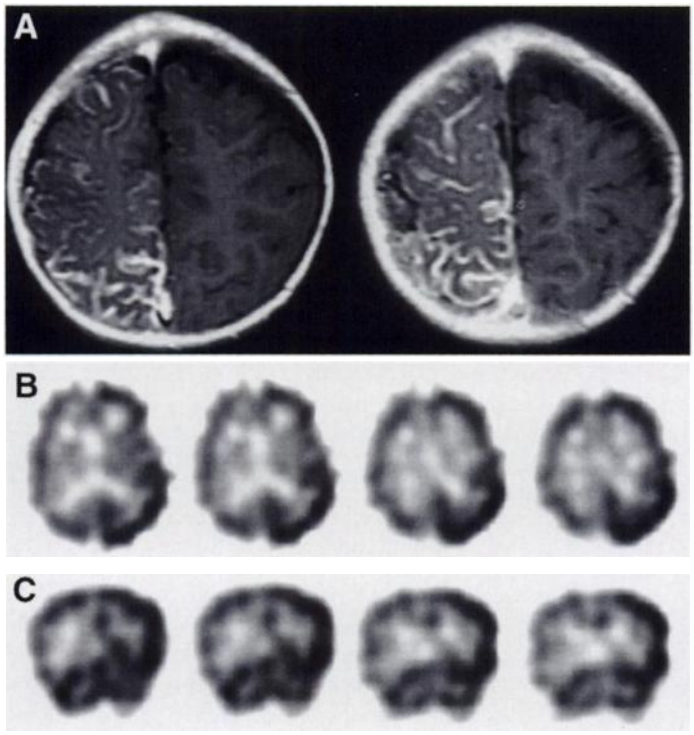

FIGURE 2. Gadolinium-enhanced, T1-weighted axial MRI (A) demonstrates right frontoparietal cortical atrophy and enhancement. Transverse (B) and coronal (C) ^{99m}Tc-HMPAO SPECT reveal globally diminished tracer localization in the right cerebral hemisphere.

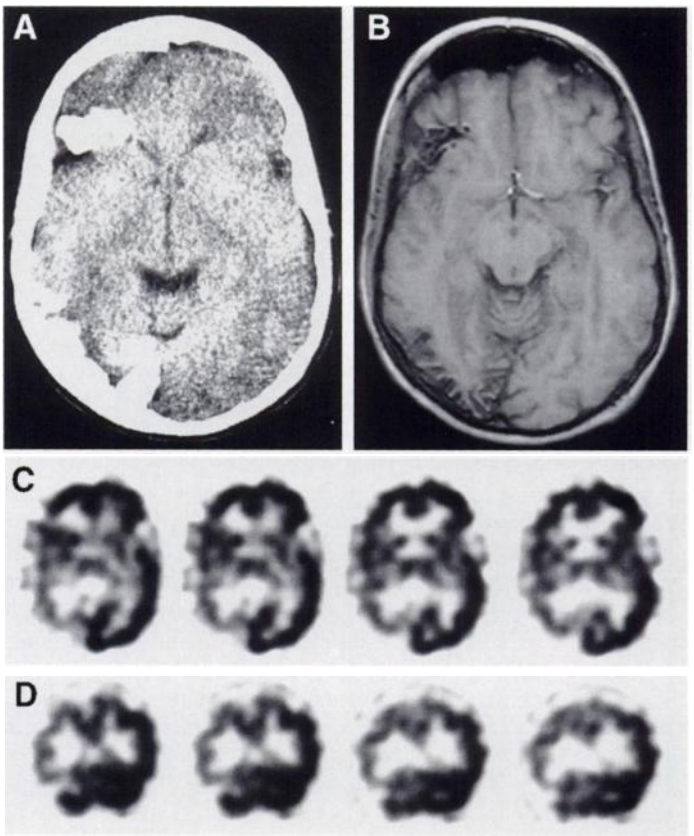

FIGURE 3. Nonenhanced CT (A) and axial T1-weighted MRI (B) show calcifications in the posterior right frontal, temporal and parieto-occipital cortex. Transverse (C) and coronal (D) ^{99m}Tc-HMPAO SPECT reveal diminished uptake in the right occipital, parietal and posterior frontal cortex.

DISCUSSION

The pial angioma of SWS represents persistence of embryonic venous plexuses. The angioma consists of dilated thin walled veins that extend beyond the macroscopically visible lesion. Some of these veins are thrombosed. Abnormal vessels may also be present in the ipsilateral choroid plexus. The pial angioma is associated with abnormal venous drainage of the ipsilateral cerebral hemisphere. The superficial cortical veins are scarce and drain into the deep cerebral veins rather than into the superior sagittal sinus. The result of these changes is vascular stasis and chronic cortical ischemia extending beyond the area that underlies the angioma. Prolonged seizures are thought to cause injury by imposing an increased metabolic demand that cannot be met by the inadequate perfusion. Further damage is inflicted by thrombotic episodes related to vascular stasis (*2,3,6,7*).

Cortical atrophy is common on the side of the angioma. This is shown by CT or MRI (*3,7–10*). Characteristic gyriform calcifications most commonly involve the occipital and posterior parietal lobes and less frequently the temporal and frontal lobes. Histologically, these calcifications are located in the outer layers of the cerebral cortex and occasionally extend into the white matter (*6,11*). The calcifications are often better shown by CT than MRI.

Kuhl et al. first reported the application of radionuclide imaging to SWS in 1972 (*12*). They used [^{99m}Tc] pertechnetate and observed reduced perfusion of the affected hemisphere and corresponding tracer retention. These findings were attributed to vascular stasis and disruption of the blood-brain barrier. Evaluation of regional cerebral blood flow with ^{133}Xe SPECT has also demonstrated marked cortical and subcortical hypoperfusion to the affected hemisphere (*13*). Technetium-99m-HMPAO perfusion brain SPECT in our patients and in one other report (*14*) have revealed interictal hypoperfusion of the affected hemisphere.

Decreased regional or hemispheric glucose metabolism was the most common FDG-PET finding in six SWS patients studied by Chugani et al. (*15*). This was believed to result from chronic ischemia and antecedent seizure activity. In one infant, however, FDG-PET demonstrated interictal hypermetabolism in the involved hemisphere. In a second infant, interictal FDG-PET showed hypermetabolism in the affected hemisphere and the contralateral cerebellum. It was postulated that this phenomenon reflects neuronal instability from chronic ischemia resulting in nonepileptiform activation of certain neuronal circuits (*15*).

The interictal SPECT pattern observed in our three patients is one of decreased ^{99m}Tc HMPAO localization in the involved cerebral hemisphere relative to the contralateral hemisphere. We believe this finding is related predominantly to the chronic cortical ischemia described above. Although perfusion or metabolic changes related to prior seizure activity (*16,17*) may also contribute to the etiology of this pattern, none of our patients were studied within 6 hr of clinically apparent seizure activity.

CONCLUSION

In our patients, as well as in those reported by others, radionuclide examination demonstrated abnormalities that are at least equally extensive as those detected by structural imaging studies. Technetium-99m-HMPAO SPECT in one of our patients revealed more diffuse hemispheric hypoperfusion than was depicted by MRI. The reported comparisons of ^{133}Xe SPECT (*13*) and FDG-PET (*15*) with CT also included patients in whom a radionuclide examination depicted a more extensive abnormality than that observed on CT or an abnormality when CT was negative.

Technetium-99m-HMPAO SPECT may provide complementary or additional information to that obtained from other imaging modalities in patients with SWS. The limited number of patients reported here prevents us from establishing the relative roles of SPECT, MRI and CT in the evaluation of SWS. These cases do, however, illustrate the cerebral perfusion abnormalities associated with SWS and contribute to an understanding of the pathophysiology of this rare syndrome.

REFERENCES

1. Ito M, Sato K, Ohnuki A, Uto A. Sturge Weber disease: operative indications and surgical results. *Brain Dev* 1990;12:473–477.
2. Berg BO. Current concepts of neurocutaneous disorders. *Brain Dev* 1991;13:9–20.
3. Roach ES. Neurocutaneous syndromes. *Pediatr Clin North Am* 1992;39:591–620.
4. Bebin EM, Gomez MR. Prognosis in Sturge-Weber disease: comparison of unihemispheric and bihemispheric involvement. *J Child Neurol* 1988;3:181–184.
5. Arzimanoglou A, Aicardi J. The epilepsy of Sturge-Weber syndrome: clinical features and treatment in 23 patients. *Acta Neurol Scan Suppl* 1992;140:18–22.
6. Di Trapani G, Di Rocco C, Abbamondi AL, Caldarelli M, Pocchiari M. Light microscopy and ultrastructural studies of Sturge Weber disease. *Child's Brain* 1982;9:23–36.
7. Terdjman P, Aicardi J, Sainte-Rose C, Brunelle F. Neuroradiological findings in Sturge-Weber syndrome and isolated pial angiomatosis. *Neuropediatrics* 1990;22: 115–120.
8. Elster AD, Chen MYM. MR imaging of Sturge-Weber syndrome: role of gadopentetate dimeglumine and gradient-echo techniques. *Am J Neuroradiol* 1990;11:685–689.
9. Sperner J, Schmauser I, Bittner R, et al. MR imaging findings in children with Sturge-Weber syndrome. *Neuropediatrics* 1990;21:146–152.
10. Lipski S, Brunelle F, Aicardi J, Hirsch JF, Lallemand D. Gd-DOTA enhanced MR imaging in two cases of Sturge Weber syndrome. *Am J Neuroradiol* 1990;11:690–692.
11. Norman MG, Schoene WC. The ultrastructure of Sturge Weber disease. *Acta Neuropathol (Berlin)* 1977;37:199–205.
12. Kuhl DE, Bevilacqua JE, Mishkin MM, Sanders TP. The brain scan in Sturge Weber Syndrome. *Radiology* 1972;103:621–626.
13. Chiron C, Raynaud C, Tzourio N, et al. Regional cerebral blood flow by SPECT imaging in Sturge Weber disease: an aid for diagnosis. *J Neurol Neurosurg Psychiatry* 1989;52:1402–1409.
14. Ton-That QT, Picard D, Bisson-Doyal D, Soucy JP, Carrier L. Technetium-99m-HMPAO imaging in Sturge-Weber syndrome. *Clin Nucl Med* 1990;15:178–180.
15. Chugani AT, Mazziotta JC, Phelps ME. Sturge Weber syndrome: a study of cerebral glucose utilization with positron emission tomography. *J Pediatr* 1989;114:244–253.
16. Rowe C, Berkovic S, Sia S, et al. Localization of epileptic foci with postictal single photon emission computed tomography. *Ann Neurol* 1989;26:660–668.
17. Rowe C, Berkovic S, Austin M, et al. Patterns of postictal cerebral blood flow in temporal lobe epilepsy: qualitative and quantitative analysis. *Neurology* 1991;41: 1096–1103.